ELSEVIER

Journal of Hydrology 198 (1997) 226–244

Journal of Hydrology

Inverse modelling of seawater intrusion in the Llobregat delta deep aquifer

V. Iribar[a,*], J. Carrera[b], E. Custodio[b], A. Medina[b]

[a]*Euskal Herriko Unibertsitatea/Universidad del País Vasco, Faculty of Sciences, P.O. Box 644, E-48080 Bilbao, Spain*

[b]*Universitat Politècnica de Catalunya, Depatment of Ground Engineering (ETSECCP) and International Centre for Groundwater Hydrology, Gran Capità s/n, Modul D.2. E-08034 Barcelona, Spain*

Received 21 March 1996; revised 4 October 1996; accepted 4 October 1996

Abstract

A flow and mass transport mathematical model has been calibrated to simulate piezometric head and chloride evolution in the Llobregat delta confined aquifer. A twenty-year period (1965–1985) is simulated with monthly time steps. Automatic estimation of flow and transport parameters are obtained by means of a code that simulates flow and mass transport of constant density fluids. In this case, density differences owing to groundwater salinity changes by marine intrusion can be neglected because the aquifer thickness is relatively small and because both the horizontal density gradient and the aquifer dip are small. Calibration of the flow problem leads to an excellent fit between measured and computed heads, which, however, can be obtained with different transmissivity patterns. When switching to the transport problem, best results in terms of concentration fits are obtained by associating the seawater intrusion plumes with high transmissivity zones that can be attributed to palaeochannels. In short, transient head and concentration data have been used jointly for automatic calibration of a regional model, which has proven advantageous both because it facilitates model selection and because it has led to a model with an improved conceptual basis.

1. Introduction

The Lower Llobregat aquifer system is formed by the Lower Valley and Delta aquifers located a few kilometers S.W. of Barcelona (Spain). Their age is Quaternary and they extend over about 100 km^2 (Fig. 1(A)). The Lower Valley (Fig. 1(A)) aquifer is formed

* Corresponding author.

PII S0022-1694(96)03290-8

from coarse gravels and sands. This formation continues below the present morphological delta towards the coast. To the delta sides the aquifer materials change to sediments from local creek alluvial fans and beach deposits. The deep delta aquifer is formed by these deposits and the deep formation shown in Fig. 1(B). Geophysical data show that this layer, with decreasing thickness, extends seaward and outcrops (directly or through a thin cover of younger sediments) at the sea bottom, about 4–5 km offshore and around the 100 m isobathe, (Serra and Verdaguer, 1983). The paper refers only to this deep aquifer.

The deep delta aquifer is confined by clay, silt and fine sand wedge-shaped sediments (Manzano et al., 1992). These sediments act as an aquitard that exhibits a very low vertical permeability, sandy sediments occur on the fringes of the aquifer. The aquitard is covered by sands, gravels and silt. This set constitutes the shallow delta aquifer, mostly a water-table one. It has some hydraulic continuity with the deep delta and the lower valley aquifers in the fringes of the delta. The Lower Valley and the deep aquifers have been intensively exploited for groundwater since the turn of the century and especially since 1950. This has produced a potentiometric depression in its central part (Fig. 1(B)) and the salinization of 30% of the confined aquifer below the delta area. The following essential points are to be considered.

1. The whole Lower Valley is a recharge area, the water table is permanently held below the river channel level, and river water infiltration passes through the unsaturated zone. Part of this recharge is pumped out by local wells and the remainder flows to the deep delta aquifer, where it is extracted, especially in the central area, leading to the depressed potentiometric heads in the central part of the delta.
2. Wells near the deepest part of the potentiometric depression receive water from both sides, that is to say, recharge from the Lower Valley and groundwater coming from the sea side.
3. Vertical head gradients in the aquitard favour downward flow from the shallow aquifer. This flow is only significant through sandy areas at the delta sides.

The displacement of the 1000 mg l^{-1} Cl^- contour line is deduced by comparing the time evolution of chloride content in numerous wells and piezometers (Fig. 1(C)). Seawater has penetrated inland from the coast following three preferential paths. The plumes point to the main extraction wells of the delta. They are related to sedimentological features of the delta. The plume in the central part of the delta intrudes through a high permeability zone, which coincides with the pre-glaciation palaeovalley of the Llobregat river. The connection with the sea is located 5 km seawards, at a depth of 100 m. At the eastern boundary of the delta the deep aquifer is covered by a sandy formation, and sea water penetration is only hindered by the thin muddy deposits on the sea bottom. At the S. W. delta boundary, highly saline water already existed in 1965, over about 2 km^2. It was identified as the remnants of an unfinished flushing of marine water by freshwater (Custodio, 1981). The lowland altitude did not allow enough freshwater head to flush out the marine water, even before aquifer exploitation started. Present-day abstractions along the inner boundary have reversed the process and saline water has penetrated towards the main wells of the area. In that zone, the aquifer becomes unconfined, and brackish water can penetrate directly from the coastal zone. Two of the plumes merge at the delta centre, leaving a freshwater pocket surrounded by saline water. The surface

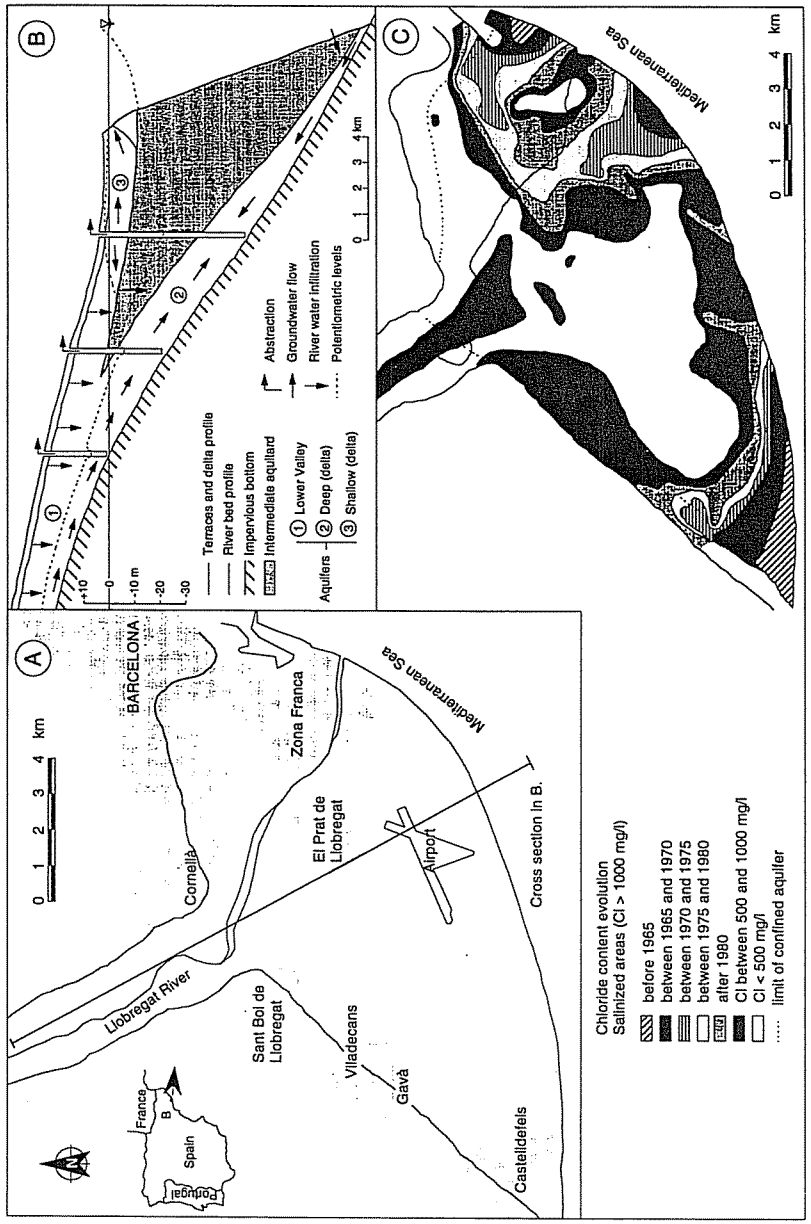

Fig. 1. (A) location of the area studied; (B) schematic flow pattern of the aquifer system coherent with hydrodynamic and hydrochemical data; (C) chloride content evolution in the deep aquifer.

area of this pocket of freshwater has progressively decreased owing to groundwater abstractions inside it.

A very wide saltwater–freshwater mixing zone with little or no vertical salinity stratification has been produced owing to the following factors.

High aquifer permeability and dispersivity (heterogeneity).
Small aquifer thickness (about 5 m) relative to the flow path lengths.
A long displacement of saline water inside a confined area without flushing.

Since the aquifer is an important supply source and an emergency reserve, different mathematical models have been used at different times to help in defining management strategies. Around 1970, the Water Administration built a model of groundwater flow in the Lower Llobregat aquifer system (Cuena and Custodio, 1971), consisting of two layers connected through an aquitard. The model was calibrated with four years of data, at three-month time-steps, and adapted to the small capacity computers then available. In 1985, a mathematical flow model for the Lower Llobregat aquifer system was prepared (PHPO, 1985), based on the code of Trescott (1975). The model was calibrated with a quarterly data-set of five years and validated with a yearly data-set of 17 years. It was used to study the effect of a series of aquifer exploitation alternatives. In 1989, a flow and transport model for the Llobregat deep delta aquifer was prepared (Custodio et al., 1989), starting with data from the previous model. The USGS MOC code (Konikow and Bredehoeft, 1978) was used. Mass transport was calibrated with a set of four years of data. Several management alternatives on seawater intrusion control for a 20-year period were studied. These models suffered from several drawbacks. They did not take full advantage of a long record of existing data, and they did not adequately explain the shape of saltwater intrusion plumes. Therefore, the objective of our work is to build a model that overcomes these limitations.

The new flow and transport model explained here has been constructed to integrate existing potentiometric and salinity data since 1965 (Iribar, 1992). This provides a long calibration period. It has also provided a test for automatic flow and transport parameter estimation offered by the new code TRANSIN II (Medina and Carrera, 1996). Automatic calibration of a model by joint use of head and concentration data is still rare. In fact, we do not know of any model automatically calibrated for transient flow and transport. Therefore, this paper emphasizes the automatic calibration aspects of the modelling effort. As a consequence, the paper is organized as follows. We start by describing the code TRANSIN II, and then continue with the conceptual model. This is modified during the calibration process, which is presented next. The paper ends with a discussion of the final model and the methodology adopted.

2. Description of the code

2.1. Flow and solute transport equations

The TRANSIN II code has been developed for the simulation of groundwater flow and solute transport under a wide range of assumptions. The forms adopted in this study are

discussed below. Groundwater flow is controlled by:

$$\nabla-(T\nabla h)+w(h)=S\frac{\partial h}{\partial t} \quad on\ \Omega \tag{1}$$

where T is the transmissivity tensor [L^2T^{-1}]; h is the head [L]; ∇ is the "del" operator [L^{-1}] (divergence or gradient); S is the storage coefficient; t is time [T] and $w(h)$ is a distributed sink/source term [LT^{-1}], which in this case is given by:

$$w(h)=\alpha(h-H)+r \tag{2}$$

where α [T^{-1}] is the leakage factor controlling inflows (outflows) from an aquitard (α equals hydraulic conductivity divided by aquitard thickness); H [L^{-1}] is the prescribed head in the upper aquifer and r is areal recharge [LT^{-1}] (both H and r may be time dependent).

Eq. (1) is solved in the domain Ω, subject to appropriate boundary and initial conditions. Time-dependent prescribed head, prescribed flow and mixed boundary conditions were used in this study.

Because of the nature of the medium and solute, only advection and dispersion are considered as relevant transport mechanisms. Therefore, the solute transport equation written in a vertically integrated form is:

$$\nabla(bD\nabla c)-\nabla(bqc)+wc_e=b\frac{\partial\phi c}{\partial t} \quad on\ \Omega \tag{3}$$

where c_e is the concentration of water entering the aquifer (c_e equals c for the discharging portions of the aquifer); q is the water flux [LT^{-1}]; D is the dispersion coefficient tensor [L^2T^{-1}]; b is the aquifer thickness [L], and ϕ is the effective porosity. Eq. (3) is solved subject to appropriate boundary and initial conditions. The former accounts for lateral sinks and sources.

Eqs. (1), (2) and (3) are solved using the Finite Element Method in one, two or quasi-three dimensions. Further details of these equations are given by Bear (1972). It should be noticed that the code does not handle density variations or density-driven flow.

2.2. The inverse problem

The inverse problem (automatic calibration) consists of finding the values of model parameters (transmissivity, porosity, parameters controlling boundary conditions, etc.) that grant a good reproduction of head and concentration data, and are consistent with prior independent information. Formulation of the inverse problem can be based on different rationales (Carrera and Neuman, 1986; Carrera, 1987). The approach implemented here is based on maximum likelihood estimation, which leads to finding the parameters that minimize an objective function of the form:

$$J=J_h+\lambda_cJ_c+\sum_i\lambda_iJ_i \tag{4}$$

where

$$J_h=(h-h^*)^tV_h^{-1}(h-h^*) \tag{5}$$

$$J_c=(c-c^*)^tV_c^{-1}(c-c^*) \tag{6}$$

$$J_i=(p_i-p_i*)^tV_i^{-1}(p_i-p_i^*) \tag{7}$$

h^* and c^* are the vectors of head and concentration measurements, whose dimensions are n_h and n_c, respectively; p_i*) is the vector (n_i dimensional) of prior estimates of type i model parameters (i identifies the type of model parameters; $i=1$ for transmissivity, $i=2$ for storativity, etc); V_h, V_c and V_i are their respective covariance matrices and λ_c and λ_i are relative weighting coefficients. These coefficients are used for giving varying weights to the different pieces of information. Minimization of Eq. (7) is achieved by the Marquardt method.

In summary, input data consists of that which is required for standard simulation problems (i.e. the finite element grid, boundary conditions, etc.) plus head and concentration measurements and prior estimates of model parameters (i.e. guesses at the values of transmissivity, recharge, etc.) as well as information relative to the reliability of these data. Automatic calibration is not as simple as might be suggested by this section. It is complicated by conceptualization difficulties. The initial conceptualization derived by the modeller is rarely satisfactory. When calibrating the model, one is usually forced to revise the initial assumptions, often in the direction of increasing their complexity and the number of model parameters.

3. Conceptual model and data input

The model was applied only to the deep delta aquifer. This, together with the fact that concentrations are well mixed in the vertical direction and that the thickness is small compared to horizontal extent, supports the use of a two-dimensional horizontal model. Modelling sea water intrusion by means of a two-dimensional horizontal model is somewhat unusual. Most models (see de Breuck, 1991; Custodio and Bruggeman, 1987) are either vertical cross-sections or fully three-dimensional. The vertical component is required to properly account for buoyancy caused by density differences. Since this effect is negligible in the deep Llobregat delta aquifer, a two dimensional, Dupuit-type model is acceptable. Two-dimensional horizontal models can still take density variations into account. In fact, they are often used to locate sharp fronts (see Custodio and Bruggeman, 1987 for a review). However, in the case under study, the front is well mixed. Therefore, it would be adequate to work with the following form of Darcy's law.

$$q=\frac{k}{\mu}(\nabla p+\rho g\nabla z)=\frac{k\rho_f g}{\mu}\left[\nabla h_f+\frac{(\rho-\rho_f)\nabla z}{\rho_f}\right] \tag{8}$$

where q is flux [LT^{-1}]; k is intrinsic permeability [L^2]; μ is viscosity [$ML^{-1}T^{-1}$], p is pressure [$ML^{-1}T^{-2}$]; z is elevation [L]; h is head [L]; g is acceleration of gravity [LT^{-2}], ∇ is the "del" operator [L^{-1}] (divergence or gradient), ρ is water density [ML^{-3}] and the subindex f stands for fresh water. By working with the conventional flow Eq. (1) using h_f, the equivalent freshwater head, the term $(\rho-\rho_f)\nabla z/\rho_f$ is neglected. Considering that the concentration in the inland part of the model rarely exceeds 3 g l^{-1} Cl^- ($\rho < 1.0025$ kg l^{-1}) and that ∇z does not exceed 0.003, $(\rho-\rho_f)\nabla z/\rho_f$ does not exceed 10^{-5}, which is small compared to ∇h_f (normally above 10^{-3}). Obviously, spurious effects should be expected in the off-shore portion of the aquifer (which is included only to

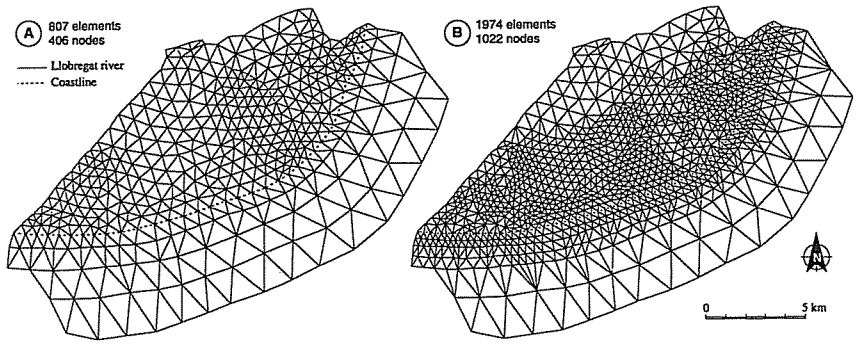

Fig. 2. Model grids: (A) for the flow problem; (B) for the flow and mass transport problem.

provide a boundary) and at unknown areas of sharp topography (large ∇z). Otherwise, accounting for density variations would add little to the model.

The flow problem uses a finite element grid of 436 nodes and 807 elements (Fig. 2(A)). To solve the flow-and-transport problem, an automatic grid refinement code was used in order to simulate the saline intrusion plumes (Fig. 2(B)) with more accuracy and fewer numerical problems. The model characteristics, the results from the best flow run (called FLOW), and the two best flow and mass transport runs (called FT-1 and FT-2) are presented in this paper.

It is assumed that the aquifer boundaries are impermeable except where the aquifer contacts the sea and the Lower Valley aquifer (Fig. 3(A)). Constant level and concentration boundary conditions are imposed there. Since the model works with equivalent fresh-water heads, the constant water-level at the aquifer–sea connections was fixed at +2.5 m at the centre (100 m depth) and at +1.5 m at the sides (60 m depth). At the connection with the Lower Valley, well known historical water levels and concentrations were applied (Fig. 3(B)). This boundary leaves most of the unconfined portion of the aquifer out of the modelled region, so that input data is restricted to transmissivities (i.e. thickness remains constant over time). A further advantage of adopting this boundary is that it avoids the simulation of river water recharge along the river channel and at the irrigated fields in the Lower Valley.

The connection of the deep delta aquifer with the shallow delta aquifer through the aquitard is simulated by introducing a leakage condition into the connecting nodes. Throughflow between the two aquifers [L^3T^{-1}] is represented at each node by α_n (h_1-h_0) in which h_1-h_0 [L] is the water head difference between the two aquifers, $\alpha_n = k'al^{-1}$ is the leakage coefficient [L^2T^{-1}], k' is the aquitard vertical permeability [LT^{-1}], a is the surface area associated with the node [L^2] and l is the aquitard thickness [L]. Leakage zones have been defined according to the aquitard vertical permeability. Four areas of uniform permeability but varying aquitard thickness have been considered (Fig. 3(A)). Table 1 contains the k' values used in the last runs. Leakage water concentration was assumed to be 300 mg l^{-1} Cl^- because the deeper part of the aquitard has been partially flushed of connate marine water (Peláez, 1983; Iribar and Custodio, 1992), and no salt

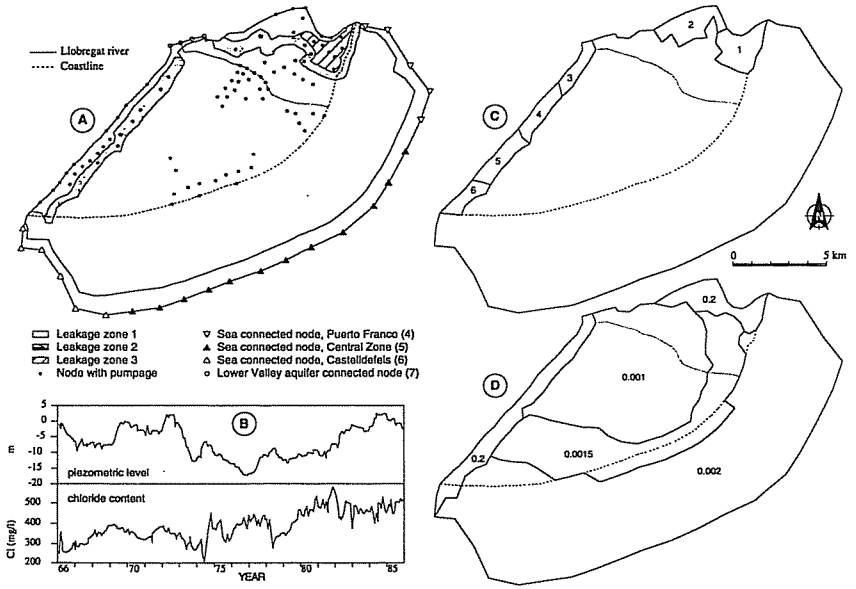

Fig. 3. Model zones and boundary conditions: (A) location map of leakage, pumping and fixed head nodes; (B) groundwater head and chloride content versus time at the connection between the deep delta aquifer and the Lower Valley aquifer; (C) zone number for recharge from the surface (see Table 1); (D) values of storage coefficient.

water reaches the aquitard bottom during the simulation period. The shallow delta aquifer water level has been considered constant because actual fluctuations are small compared to those observed in the deep aquifer. A value of +1 m has been given to inland nodes and +1.2 m to offshore nodes.

Groundwater pumping was simulated as a prescribed sink term over sets of several nodes (Fig. 3(A)). This is a consequence of two facts. First, the density of wells is very high, so that the grid cannot take all of them into account. Second, most pumping data refers to clusters of wells, rather than individual ones. As a result, pumping nodes have been grouped in "zones" which differ from each other in their pumping history. A total of 56 zones were considered.

Table 1
Characteristics of the leakage zone areas (see Fig. 3(A) for geometry of zones)

Leakage zone number	FLOW	k' (m per day) in runs FT-1	FT-2	Fixed head altitude (m)
1	0.25E-7	0.25E-7	0.25E-7	+1.0
1	0.25E-7	0.25E-7	0.25E-7	+1.2
2	0.13E-2	0.13E-2	0.28E-2	+1.0
3	0.11E-1	0.11E-1	0.70E-2	+1.0

Table 2
Recharge from the surface (see Fig. 3(C) for geometry of zones)

Zone number	Area (km^2)	Recharge (mm per day) in runs		
		FLOW	FT-1	FT-2
1	4.62	0.44	0.66	0.50
2	4.39	1.60	1.52	1.50
3	1.92	2.00	1.50	1.50
4	2.35	1.70	1.28	1.50
5	2.85	1.46	1.98	1.50
6	1.94	1.83	1.39	1.50

Direct recharge from the surface is only possible at the delta boundaries, where the aquitard thins out. This recharge is due to local rainfall, to excess irrigation water infiltration, to losses from irrigation canals, to leakage from supply and sewer networks and to contributions from the small tributary basins at the sides (lateral flow). Since the detailed evaluation of all these contributions is too complex, six zones have been distinguished according to the geographical location, two at the delta eastern sector and four at the western sector (Fig. 3(C)). Recharge has been considered uniform and constant within each zone. Values adopted in the final calibration stages are about 360 mm per year (Table 2). A salinity of 300 mg l^{-1} Cl^- is assumed for this recharge.

Zones for the storage coefficient are shown in Fig. 3(D). High values are adopted at the aquifer boundaries, for the stripes where the intermediate aquitard is absent, whilst low values are given to the confined part.

Three different transmissivity zone patterns have been used during the calibration process (Fig. 4). Distribution A was that of the PHPO (1985) mathematical flow model. Distribution B was prepared after the isotransmissivity map from PHPO (1985), which is

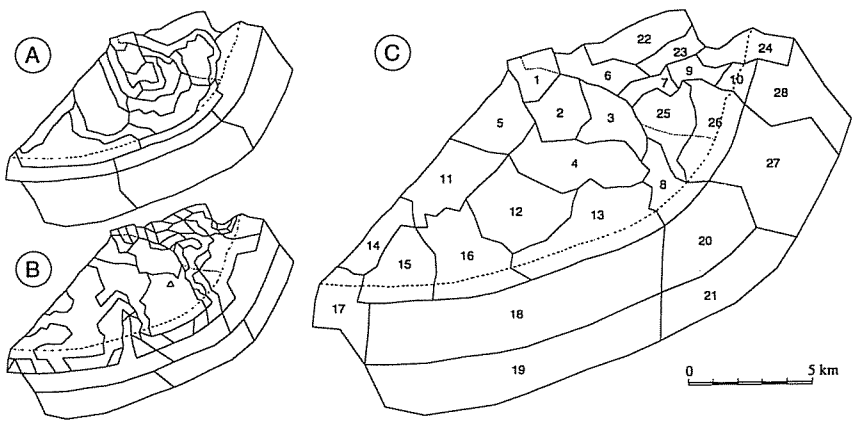

Fig. 4. Transmissivity zones used in the model: (A) adapted from PHPO (1985) model; (B) adapted from MOP (1966) model; (C) last distribution used in this model with better results; the figures in it indicate its numbering.

Table 3
Transmissivity values in m^2 per day as adopted in the last runs (see Fig. 4(C))

Zone number	FLOW	FT-1	FT-2	Zone number	FLOW	FT-1	FT-2
1	31077	17840	33270	15	1442	540	61
2	21984	30710	19180	16	827	4051	574
3	16851	4819	2091	17	923	5912	192
4	6998	5190	7619	18	590	916	4.53
5	2067	8500	4655	19	54	4E − 05	278
6	4036	22420	9019	20	9898	9E + 09	461
7	3140	9441	27840	21	521	5.68	1.90
8	16821	1E + 10	6E + 08	22	391	67	290
9	2881	1369	4971	23	105	873	222
10	2916	159	3697	24	873	6423	5872
11	1188	832	1134	25	205	54	1085
12	1000	2831	1000	26	100	2020	6.43
13	425	231	572	27	1.35	121	0.45
14	254	3E + 09	1226	28	3E − 03	0.85	8.87

the result of the combination of pumping tests and specific well discharges. Distribution C was adopted after the first results of the calibration process. The final values were adjusted during the late calibration stages and are given in Table 3.

Other parameters have been used in the model. Effective transport porosity was fixed at 0.20. Longitudinal and transverse dispersivity coefficients were taken as 400 and 200 m respectively. Smaller values would have been needed for representing small-scale features of the concentration front. However, adopted values are consistent with the scale of the model (see Carrera, 1993 for a discussion). A value of 0.001 m^2 per day was given to molecular diffusivity, although it barely affects the simulation.

The simulation period is from January 1966 to December 1985, that is to say, 20 years. In 1965, the delta monitoring piezometer network was established and an extensive groundwater sampling survey was carried out. This allows a good definition of initial conditions. Pumping values from that time to 1983 were available from the PHPO (1985) model, later extended in 1985 by the Water Authority of Catalonia. Since a further extension required a good deal of work, it was decided to end the calibration period then, instead of carrying out dubious extrapolations. Owing to the fact that there was very little potentiometric data in December of 1965, the July 1965 potentiometric surface (Fig. 5), taken from MOP (1966), has been used as the initial condition. Offshore heads represent an extrapolation from inland values. The isochloride map of December 1965 (MOP, 1966) was adopted (Fig. 5) as the Cl^- concentration initial situation, also by extrapolating the inland values to the offshore part of the aquifer.

The 20 year simulation has been carried out with one-month time-steps. Thus, the total number of time steps is 240. This proved sufficient for accuracy (recall that pumping was distributed over clusters of wells and that no attempt was made at simulating responses to individual wells). Moreover, it facilitated comparison of model computations with groundwater level records from the Catalonia Water Authority monitoring network, mostly measured monthly.

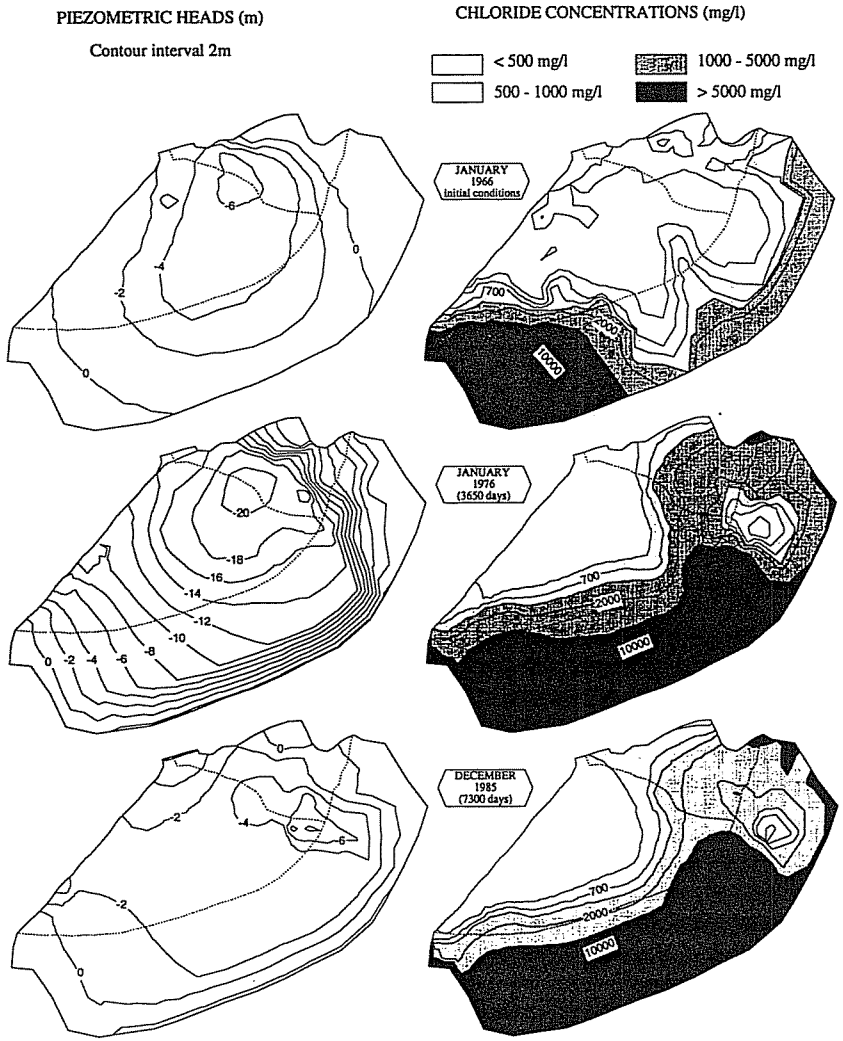

Fig. 5. Time evolution of groundwater heads (m) for the FLOW run and concentrations (mg l^{-1} Cl^-) for the FT-2 run.

4. Calibration

Parameter values are updated by zones during the calibration process. When results were not satisfactory, the zonation pattern was modified and a new calibration process was initiated. Adjustments were carried out both by hand and automatically. Automatic adjustments were carried out by TRANSIN II, starting with the parameters selected. As

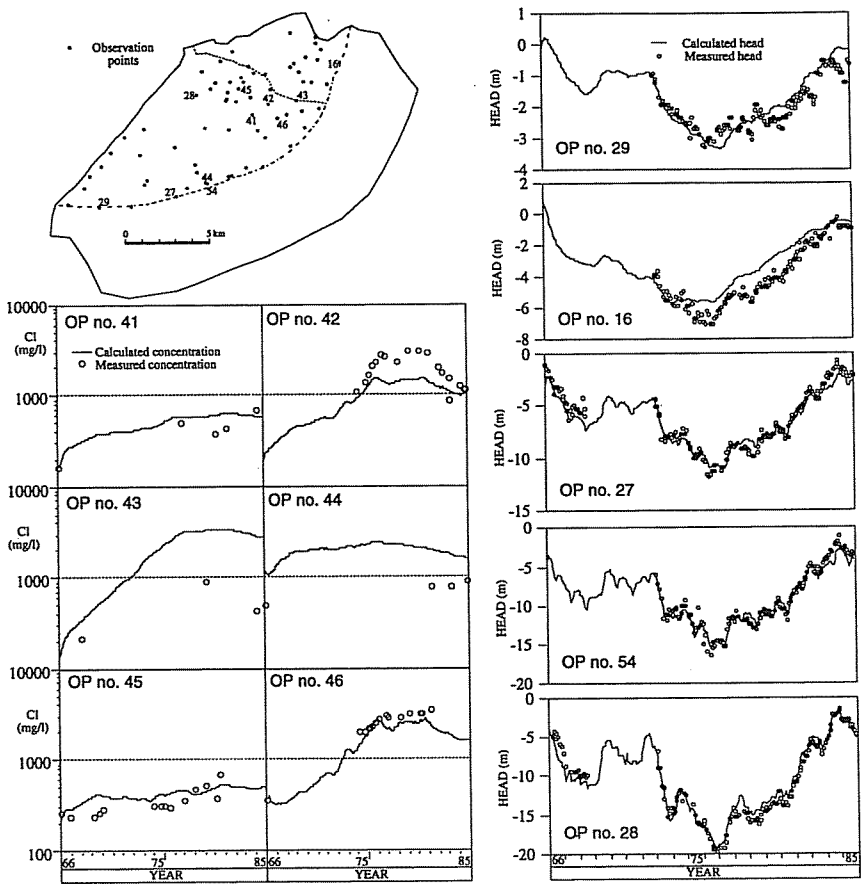

Fig. 6. Time evolution of groundwater head and concentrations at selected observation points.

explained before, the code minimizes an objective function, J, with respect to the model parameters representing aquifer properties. This objective function considers the differences between measured and calculated heads and/or concentrations, as well as the likelihood of calculated parameters (Carrera, 1990). Therefore, unlike in standard simulation codes, TRANSIN II needs measured heads and concentrations at what are defined as observation points. As shown in Fig. 6, observation points provide a good coverage of the model domain. The number of observations is 3937 for heads and 667 for Cl^- concentrations, a total of 4604 observations. Head data at most observation points extends over the whole calibration period (with a few wells lacking data prior to 1972). However, the concentration data record is generally available from 1974 to 1985, although some scattered data are available from 1965 to 1974.

The transmissivity zoning A (Fig. 4), derived from the PHPO (1985) final calibration, produced rather good results for the flow problem, but was not able to simulate the seawater intrusion plumes in the mass-transport problem; the saline front penetrates uniformly towards the delta centre, without forming any plume. Therefore, it had to be modified in subsequent runs. The first modification of the transmissivity zoning was performed in agreement with the isotransmissivity map derived from pumping tests and specific well discharge (PHPO, 1985), this map includes heterogeneities that should have improved mass transport simulation (Fig. 4(B)). This change produced rather bad results since the head objective function was impaired notably and the transport solution did not improve. Therefore, new zoning for model (Fig. 4(C)) was defined according to the following criteria.

1. Differentiate specific zones to model the intrusion plumes, giving them high permeability values. These can be attributed to palaeochannels. They are known to exist and their orientation is consistent with that of the proposed zones.
2. Use of direct T measurements to delineate zones and assign prior estimates to T values.
3. For the rest, the zonation was defined on the basis of head measurement points. That is, large zones were defined in areas of low measurement density, and vice-versa.

These changes led to satisfactory results. It is important to stress that the use of automatic calibration forced the modellers to concentrate on conceptual issues, allowing them to be freed from manual calibration. Numerous runs were carried out to try to calibrate all parameters, except pumpage and the connection condition with the Lower Valley. First, the flow problem was calibrated in an acceptable form, and afterwards the grid was refined and the model calibrated for the flow and mass transport problem. Since the number of nodes and elements is high and the flow regime is transient, the flow and mass transport runs consumed a great deal of CPU time, about 4.5 days to estimate 20 parameters using an HP Alliant computer.

Runs FT-1 and FT-2 started from different sets of parameter values. The FT-1 run used, as starting parameters, those used in the best flow run (FLOW); all parameters were fixed, except the 28 transmissivity zones. FT-2 used the final FLOW parameters but slightly modified according to the results of other runs that produced good fits. The transmissivity values that changed little in these runs were fixed, mainly those near the Lower Valley connection. Transmissivity in areas close to the coast and to the boundaries was then estimated, together with leakage at the intermediate aquitard boundary and at the Zona Franca area, where the model behaviour was very sensitive. This type of handling was required to manage instability.

The values of the calibrated objective functions are shown in Table 4. The same weight (standard deviation) was assigned to all head (1 m) and concentration measurements (500 mg l^{-1}) in all runs. Therefore, the values of J_h and J_c can be compared to each other. The value of J_i is more difficult to interpret because each run was based on a different number of zones and variable standard deviations were used for each parameter. Therefore, the values of the total objective function (J) cannot be used for comparison.

It can be seen that the best head fit is obtained in model FLOW (that is, when there are no fitting of concentration). When introducing concentrations and estimating transmissivity (run FT-1), J_h was kept low, but parameter estimation became unstable, leading to

Table 4
Values of the objective functions obtained for the calibration runs (see Eqs. (4)–(7))

Run	J (4)	J_h (5)	J_c (6)	J_i (7)
FLOW	0.22E + 5	0.55E + 4	—	0.16E + 5
FT-1	0.10E + 6	0.56E + 4	0.98E + 5	0.50E − 1
FT-2	0.54E + 5	0.14E + 5	0.40E + 5	0.12E − 1

absurd values in zones 8, 14, 19 and 20 (Table 3). In fact, this was obtained at the cost of reducing the weight assigned to prior information (notice the reduction in the value of J_i in Table 4, caused by an increase in the standard deviations, that is, a large decrease in V_i, which is inverted in Eq. (7)).

When going from run FT-1 to FT-2 concentrations errors (J_c) were reduced by a factor of about 2.45, but the squared head errors (J_h) are worsened by a factor of about 2.5, which is a consequence of forcing the model to fit concentrations. It is interesting to observe that parameter estimates of run FT-2 are quite stable (Table 3), despite of the fact that little weight was assigned to them.

Fig. 6 displays the time evolution of heads and concentrations by means of contour maps. Fig. 7 shows the simulated head and concentration time evolution at some observation points.

5. Balances

Table 5 displays the mean water balances obtained from the selected calibration runs. The time evolution of inflow from the intermediate aquitard leakage, the sea and the Lower Valley are shown in Fig. 7.

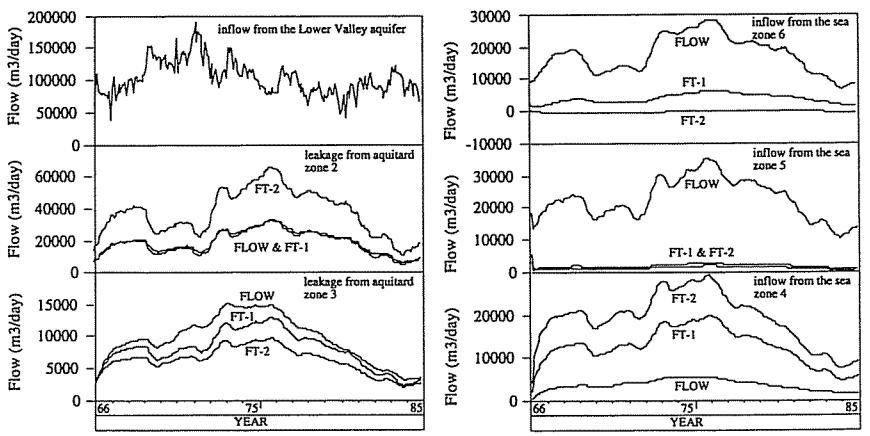

Fig. 7. Time evolution of inflow to the delta deep aquifer from the Lower Valley, from leakage through the intermediate aquifer and from the sea.

Table 5
Water balances for the last runs: mean values for the period

Zone number	m^3 per day			% of total inflow		
	FT-1	FLOW	FT-2	FT-1	FLOW	FT-2
Recharge from the surface (Fig. 3(C))						
1	3047	2031	2308	1.6	1.1	1.2
2	6669	7020	6581	3.6	3.8	3.5
3	2883	3845	2883	1.5	2.1	1.5
4	3004	3990	3520	1.6	2.1	1.9
5	5648	4165	4279	3.0	2.2	2.3
6	2695	3548	2908	1.4	1.9	1.6
Total	23946	24597	22480	12.8	13.2	12.0
Leakage from the intermediate aquitard (Fig. 3(A))						
1	2	2	2	0.0	0.0	0.0
2	18491	19397	37689	9.9	10.4	20.2
3	7903	9544	6204	4.2	5.1	3.3
Total	26395	28943	43895	14.1	15.5	23.5
Inflow from the sea (Fig. 3(A))						
4	12645	3625	19301	6.7	1.9	10.3
5	1307	22683	1924	0.7	12.1	1.0
6	17549	4047	−122	9.4	2.2	−0.1
Total	31501	30355	21102	16.8	16.2	11.3
Inflow from the Lower Valley (Fig. 3(A))						
7	105572	103059	99494	56.3	55.1	53.2
Total inflow	187414	186955	186971			
Total pumpage	187430	187430	187430			

6. Discussion

The final runs for mass transport are not as satisfactory as those for flow. This does not necessarily imply a lower quality of the calibration, since more parameters are needed for transport than for flow and thus they are subject to more uncertainty. However, this can also be attributed to the lower reliability of salinity (chloride content) data, which are much less systematic. Some data were obtained from continuously pumped wells, some from wells pumping during a short period of time and some with a grab sampler from observation boreholes under non-ideal conditions. Also the mass transport problem is highly dependent on poorly known or simply unknown local heterogeneities, whilst the flow problem can be represented by more regional parameters, which integrate heterogeneities and correspond to some extent to what is obtained by means of interference pumping tests.

Points at which concentration changes with time have been simulated more accurately are close to the connection with the Lower Valley, and to a wide zone on the northeast side of the delta and around the central intrusion plume (Fig. 6, OP numbers 41, 45 and 46).

At the Castelldefels area (Fig. 5), the calibration shows an excessive recharge from the boundary side or from leakage, and very little seawater inflow. Instead of sustained or increasing salinity, concentration decreases with time. In part, this is due to poor knowledge of aquifer properties and boundary and initial conditions in this area, which is more sensitive to the transport problem. Calibration cannot be expected to explain what is conceptually poorly known or where fluid density changes may play a significant role. However, some areas in the same sector continue to contain freshwater in simulations, in agreement with observations. These difficulties decrease when moving towards the central coastal area.

Computed concentrations between Castelldefels and the Llobregat river mouth are too large (Figs 5 and 6, OP number 44), although they generally fall below 2 g l^{-1} Cl^-. This can be attributed to the fact that the initial condition set in the offshore part of the delta, where no data are available, may have assumed a water salinity and areal extension which were too high.

Good results have been generally obtained around the central salinity plume, especially for time of arrival of the salinity front. Calculated concentrations tend to be less than observed (Fig. 6, OP number 42, 43 and 46).

Results in the salinized part of the Zona Franca are not as good as in the rest of the model. A fast salinization process followed by more-stable values has been observed (Fig. 5). This result may be a consequence of choosing a high permeability and a high recharge at this area. This leads to an excessively fast rate of salinization of the freshwater pocket between this area and the central salinity plume. This area is complex and would require a more detailed numerical and conceptual model to improve results.

Notwithstanding these problems, a good simulation has been achieved as a whole. The definition of high transmissivity zones allows reproduction of the central salinity plume and the freshwater pocket. The simulation has not achieved satisfactory results near Castelldefels (not enough seawater has penetrated) or at the Zona Franca (too much seawater has penetrated), probably owing to poor definition of boundary and initial conditions.

Recharge from the surface has a clear influence near the boundary zones, in the Castelldefels–Gava area (it clearly dilutes saline water) as well as in the Zona Franca (it decreases saline intrusion concentration). In the model, this recharge from the surface has been considered constant (300 mg l^{-1} Cl^-), although the observation of the calibration process indicates a variable value. There are no direct data to improve the situation (Table 5). Leakage from the intermediate aquitard is especially significant near the boundary areas. For run FT-2, the importance of leakage near the boundary areas is greater than recharge from the surface (Fig. 7 and Table 5). Leakage at the Zona Franca (Fig. 3(A), zone 3) has a smaller effect on the whole but clearly modifies local conditions.

It is clear that some uncertainty remains at the model boundaries. In part, this is due to insufficient data, both in terms of direct measurements of head, concentrations and transmissivity and in terms of a thorough geological model. In part, it can be attributed to limitations of the conceptual model. However, the fact that a stable fit of a 20 year record of data has been obtained, together with the error analysis (not shown here), suggests that the model is highly reliable in the central portion of the aquifer, which is critical from a supply point of view.

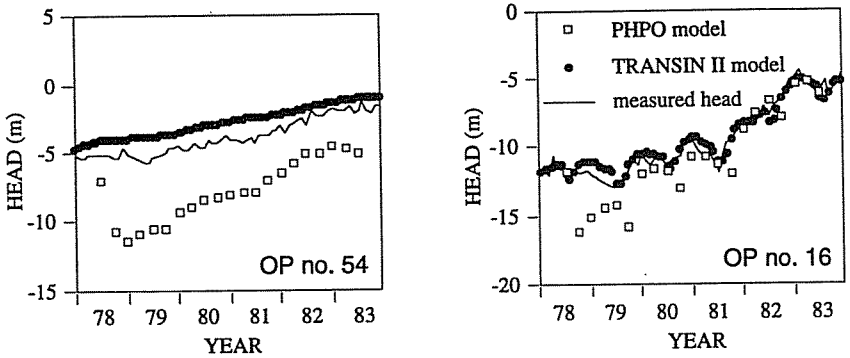

Fig. 8. Comparison between measured heads and those obtained with the TRANSIN II and PHPO (1985) models. Location of the two observation points are shown in Fig. 6.

A thorough comparison between this model and earlier models of the Llobregat delta deep aquifer would be too lengthy. For the sake of simplicity, let us just say that the final model leads to a better agreement between measured and computed heads than any of the previous models (head errors in the PHPO (1985) model, probably the best up until now, are about two times larger that in the new model, see Fig. 8). Moreover, it explains some features of the saline water intrusion that had been left unexplained by previous models. Specifically, our model reproduces the two saltwater intrusion plumes. Finally, the model explicitly accounts for palaeochannels, which are consistent with the geology of the site, but had not been taken into account earlier. All of this, together with the fact that the calibration was extended over a period of 20 years, allows us to conclude that the model is, indeed, much more robust than earlier models. It should be stressed that the main improvement, inclusion of palaeochannels, is of a conceptual nature, and has been brought about by the use of an automatic calibration technique.

7. Conclusions

The use of the TRANSIN II model has improved the flow problem simulation of the deep delta aquifer when compared with former models. A proper calibration has required the existence of high transmissivity zones where saline plumes are observed and explains the behaviour in these zones. These high transmissivity zones can be interpreted as palaeochannels. The mass transport simulation may seem less satisfactory than that of flow, which is due to the complexity of the problem, the less accurate nature of salinity data and the simplistic hypothesis of homogeneous fluid taken into account when analysing the results. However, the simulation performed is able to reproduce observed salinity trends and confirms and quantifies the conceptual model of the aquifer.

Some conclusions can also be derived regarding methodological issues. To the authors' knowledge, this is the first regional model automatically calibrated by joint use of transient head and concentration data. While at the cost of a significant computational burden, it has

had several benefits. The use of concentration data has allowed selection of a single conceptual model from a set of alternatives. While many different conceptual models led to excellent head fits, only one was able to produce a satisfactory concentration fit. The fact that, in hindsight, the resulting model is more geologically consistent than any of the others illustrates how inverse modelling allows hydrogeologists to concentrate on conceptual issues rather than devoting most of their time to the tedious task of hand calibration. From a practical point of view, this is the most important benefit of inverse modelling.

Acknowledgements

The authors thank the Water Authority of Catalonia for the use of data from its monitoring network. Also, important salinity data have been taken from the files of the Lower Llobregat Groundwater User's Community. The help needed to run the TRANSIN II programme correctly and the changes needed in the input and output have been provided by researchers at the Groundwater Group of the Department of Ground Engineering, ETSICCP-UPC, especially X. Sanchez-Vila and G. Galarza.

References

Bear, J., 1972. Dynamics of Fluids in Porous Media. Elsevier, Amsterdam, pp. 1–364.

Carrera, J. and Neuman, S.P., 1986. Estimation of aquifer parameters under transient and steady state conditions, 1: maximum likelihood method incorporating prior information. Water Resour. Res., 22(2): 199–210.

Carrera, J., 1987. State of the art of the inverse problem applied to the flow and solute transport equations. Groundwater Flow and Quality Modelling. NATO ASI Series C, 224, Reidel, pp. 549–583.

Carrera, J., 1990. A modelling approach incorporating quantitative uncertainty estimates. Water Resources in Mountainous Regions. 12th International Association Hydrogeologists Congress, Lausanne, Vol. 1, pp. 67–78.

Carrera, J., 1993. An overview of uncertainties in modelling groundwater solute transport. J. Contam. Hydrol., 13: 23–48.

Cuena, J. and Custodio, E., 1971. Construction and adjustment of a two layer mathematical model of the Llobregat Delta, Barcelona, Spain. Mathematical Models in Hydrology. UNESCO Stud. Rep. Hydrol., 15(2): 959–964.

Custodio, E., 1981. Sea water encroachment in the Llobregat and Besos areas near Barcelona (Catalonia, Spain). Intruded and relict groundwater of marine origin. Proceedings of 7th SWIM, Uppsala. Sweriges Geologiska Undersokning, Rapporter och Meddelanden, Uppsala, Vol. 27, pp. 120–152.

Custodio, E. and Bruggeman, G.A., 1987. Groundwater problems in coastal areas. UNESCO, Stud. Rep. Hydrol., 45: 1–596.

Custodio, E., Glorioso, L., Manzano, M. and Skupien, E., 1989. Evolución y alternativas de un acuífero sobreexplotado: el delta del Llobregat. Sobreexplotación de Acuíferos. International Association of Hydrogeologists (Grupo Español)-AEHS, Almería, pp. 207–227.

de Breuck, W., 1991. Hydrogeology of salt water intrusion. IAH, Int. Contrib. Hydrogeol., 11: 1–422.

Iribar, V., 1992. Evolución hidroquímica e isotópica de los acuíferos del Baix Llobregat. M.S. Thesis, Universitat de Barcelona.

Iribar, V. and Custodio, E., 1992. Advancement of seawater intrusion in the Llobregat delta aquifer. In: E. Custodio and A. Galofre (Editors), SWIM Study and Modelling of Saltwater Intrusion into Aquifers. CIMNE-UPC, Barcelona, pp. 35–50.

Konikow, L.F. and Bredehoeft, I.D., 1978. Computer model of two dimensional solute transport and dispersion in groundwater. U.S. Geological Survey Book 7. Chapter C-2.

Manzano, M., Custodio, E. and Carrera, J., 1992. Fresh and salt water in the Llobregat Delta aquifer: application of ion chromatography theory to the field data. In: E. Custodio and A. Galofre (Editors), Study and Modelling of Saltwater Intrusion into Aquifers. CIMNE-UPC, Barcelona, pp. 207–228.

Medina, A. and Carrera, J., 1996. Coupled estimation of flow and solute transport parameters. Water Resour. Res., 32(10): 3063–3076.

MOP, 1966. Estudio de los recursos hidráulicos totales de las cuencas de los ríos Besós y Bajo Llobregat. Comisar ía de Aguas del Pirineo Oriental y Servicio Geológico de Obras Públicas, Barcelona, 4 Vols.

Peláez, M.D., 1983. Hidrodinámica en formaciones semipermeables a partir de la composición química y radioisotópica del agua intersticial: aplicación a los limos intermedios del delta del Llobregat. M.S. Thesis. Universitat de Barcelona.

PHPO, 1985. Modelo de simulación de los acuíferos del Bajo Llobregat. Plan Hidrológico del Pirineo Oriental. Confederación Hidrográfica del Pirineo Oriental, Barcelona.

Serra, J.; Verdaguer, A., 1983. La sedimentación holocena en el prodelta del Llobregat. X Congreso Nacional de Sedimentología, Mahón. Universidad Autónoma de Barcelona, pp. 249–151.

Trescott, P.C., 1975. Documentation of finite difference model for simulation of three-dimensional ground-water flow. U.S. Geological Survey Open File Report. pp. 75–438.

ELSEVIER

Journal of Hydrology 198 (1997) 245–259

Journal of Hydrology

Joint use of L-moment diagram and goodness-of-fit test: a case study of diverse series

Arie Ben-Zvi[a,*], Benjamin Azmon[b]

[a]*Israel Hydrological Service, P.O. Box 6381, Jerusalem, Israel*
[b]*Israel Hydrological Service, P.O. Box 33140, Haifa, Israel*

Received 12 June 1996; revised 24 September 1996; accepted 3 October 1996

Abstract

Selection of a probability distribution for annual maximum discharges was carried through exploratory and confirmatory stages. The L-moment diagram was applied first in order to screen out inappropriate candidate distributions. The Anderson–Darling test was then applied in order to examine the descriptive performance of screened distributions. The effectiveness of this two-stage procedure was studied on an ensemble of diverse annual maximum discharge series recorded in Israel. The Generalized Pareto distribution was the only one of a number of candidate distributions whose theoretical relationship between L-moments followed closely enough the actual relationships in the case study. This distribution was well fitted to about one half of the discharge series, and satisfactorily fitted to the entire ensemble. It was concluded that such a two-stage procedure, which applies quantitative measures in both stages, would reduce the subjectivity involved with the selection of a probability distribution, thus improving the credibility of predicted high discharges. © 1997 Elsevier Science B.V.

1. Purpose

Association of magnitude of high discharges with their exceedance frequency is often requested from hydrologists. This is traditionally fulfilled by use of a probability distribution which is selected with respect to its coherence with data for a region in which the site of interest is located and adapted to the properties of that site. Selection of the distribution is a process involving a number of decisions. A rational practice for reducing the effect of subjectivity on these decisions involves use of common procedures and objective techniques. These include, amongst others, widening of the region's boundaries (e.g. selection

* Corresponding author

PII S0022-1694(96)03302-1